Journal of Inclusion Phenomena and Macrocyclic Chemistry **33:** 81–97, 1999.

Inclusion of Enantiomeric Carvones in β-Cyclodextrin: a Variable Temperature ^{1}H NMR Study in Aqueous Solution

AIDA MOREIRA DA SILVA
School of Agriculture, Polytechnical Institute of Coimbra, P-3000 Coimbra Portugal

JOSÉ EMPIS
Department of Chemical Engineering, Instituto Superior Técnico, P-1096 Lisboa Codex Portugal

JOSÉ J.C. TEIXEIRA-DIAS*
Department of Chemistry, University of Aveiro, P-3810 Aveiro Portugal

(Received: 16 October 1997; in final form: 30 January 1998)

Abstract. In aqueous solution, the apparent association constant at room temperature for the 1 : 1 inclusion of S-(+)-carvone in β-cyclodextrin is double of that for R-(−)-carvone, whereas, at 45 °C, both enantiomers have association constants two orders of magnitude smaller, with the S-(+) inclusion being then slightly weaker than the R-(−) encapsulation. Calculations carried out at the molecular mechanics, AM1 and STO-3G levels confirm the preferential inclusion of the S-enantiomer and provide important clues for understanding chiral discrimination by β-cyclodextrin.

Key words: β-cyclodextrin, carvone enantiomers, molecular inclusion, chiral discrimination, apparent association constants, molecular modelling, molecular mechanics, quantum mechanics

1. Introduction

β-Cyclodextrin (cyclomalto-heptaose, β-CD) is a short, hollow, truncated cone shaped molecule, which is formed by seven α(1-4) linked gluco-pyranoses in normal chair conformations (Scheme 1) [1]. As with the other cyclodextrins, β-CD has a positive optical rotation. Both in the crystalline hydrate and in aqueous media, the β-CD molecule interacts with water molecules, some of which are removed when a guest of suitable size enters into the cavity [2]. When β-CD interacts with the enantiomers of a chiral molecule, the difference in chiral properties between host and guest affects the host-guest interaction and the stability of the inclusion, giving rise to chiral discrimination [3–6]. In addition, different degrees of fit between the guest enantiomers and the host may influence the degree of hydration of the inclusion system. Since enantiomers undergo identical solvation processes, the study of the host-guest interactions between β-CD and the enantiomers of a

* Author for correspondence.

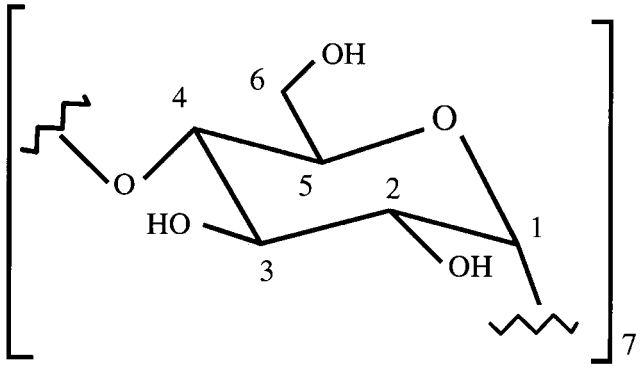

Scheme 1.

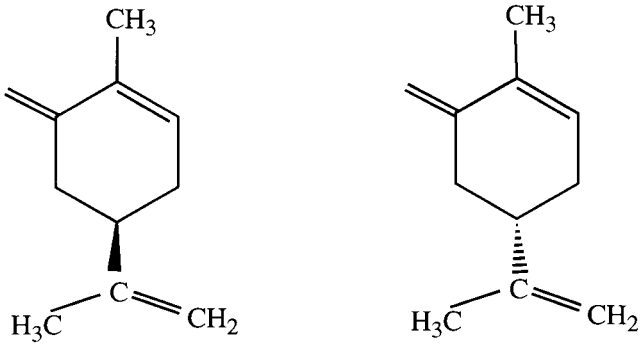

(R)-(-)-carvone (S)-(+)-carvone

Scheme 2.

chiral molecule should provide a better insight into these interactions and elucidate chiral recognition processes in biological receptor molecules [3–6]. In the past, gas-chromatographic separation of enantiomers has been achieved using alkylated cyclodextrins as chiral stationary phases in high-resolution capillary columns [3]. Cyclodextrins are also important chiral stationary phases in HPLC separations [7].

Two enantiomers of carvone (2-methyl-5-(1-methylethenyl)-2-cyclohexene-1-one, Crv) are natural components of spearmint [(R)-(−)-carvone, R-Crv] and caraway seed oil [(S)-(+)-carvone, S-Crv] (Scheme 2). As a hydrogen bond acceptor, the C=O bond of carvone can act as the anchoring group for the guest in the inclusion process, a possibility which can determine the preferential fixation of one of the enantiomers [5, 6].

The use of molecular inclusions in cyclodextrins has shown a consistent and substantial increase for a variety of reasons, ranging from increased stability and slow release of the included guest to chiral separation methodologies using cyclodextrin stationary phases [2, 7]. The case of aroma encapsulation is of particular concern if markedly different release kinetics are to alter overall perception of bou-

quet when, due to increase of temperature and water activity, such as when a food item is consumed, liberation of encapsulated flavourants occurs. Since flavours are blends of different odoriferous compounds and bearing in mind the chirality of the β-CD cavity, it was thought that the investigation of inclusions of two enantiomers would contribute to ascertain whether markedly different thermodynamic and kinetic parameters are to be expected, or if the liberation of diverse encapsulated molecules may be expected to occur at comparable rates.

In this work, the apparent association constants for the inclusion of the carvone enantiomers in β-CD are determined in D_2O solution, at different temperatures, by ^{1}H NMR. In addition, molecular mechanics and quantum mechanics calculations on model systems are carried out to help in the interpretation of the experimental results.

2. Materials and Experimental Methods

β-CD, kindly donated by Wacker-Chemie, München (Germany), was recrystallized prior to use, by cooling concentrated aqueous solutions in a Dewar flask from ca. 80 °C to room temperature. R-(−)-carvone, S-(+)-carvone, and D_2O (99.5% isotopic purity) were obtained from Aldrich, Madrid. The lower and upper temperature values used in this work (286 K and 318 K) were chosen to avoid crystallization of the inclusion compound and appreciable volatilization of carvone, respectively.

Room temperature ^{1}H NMR spectra were recorded with a 300 MHz General Electric NMR spectrometer, and the variable temperature ^{1}H NMR spectral studies were carried out using a 300 MHz Bruker MSL 300P spectrometer. D_2O was used as solvent, and the residual signal of the non-deuteriated fraction of the solvent (at 24 °C, δ = 4.8 ppm) taken as internal reference. Adequate signal-to-noise ratios were obtained by averaging the spectra over 16 or 32 scans.

The stoichiometries of the inclusion compounds were determined using a method due to Job [8] and generally known as the continuous variation method or Job's method. This method involves running a series of experiments varying the host to guest initial concentrations whilst maintaining constant the sum of the initial molar concentrations of host and guest ($[\beta\text{-CD}]_0 + [G]_0$), at well defined r values ($r = [\beta\text{-CD}]_0/\{[\beta\text{-CD}]_0 + [G]_0\}$). In particular, 10 mM D_2O solutions of the guest (G) and β-CD were mixed

(i) to constant volume, i.e., the sum of the initial concentrations of β-CD and G remained equal to 10 mM ($[\beta\text{-CD}]_0 + [G]_0 = 10$ mM), and

(ii) to defined values of r, where r took values from 1/10 to 9/10, in steps of 1/10.

The stoichiometries were finally determined by plotting $\Delta\delta.[\beta\text{-CD}]_0$ against r and finding the r values corresponding to the maxima of these distributions.

Table I. Chemical shifts (δ(ppm)) for H(5) of β-CD in a β-CD D_2O solution ($[\beta\text{-CD}]_0$ = 0.5 mM) at different temperatures

T/K	δ (ppm)
286	3.698
293	3.822
295	3.827
301	3.888
318	4.097

3. Experimental Results and Discussion

The H(3) and H(5) protons of β-CD form two inner 'crowns' of hydrogen atoms, in the wider and narrower rims, respectively. These 'crowns' of protons have strategic positions for reporting host–guest interactions in the cavity. Both H(3) and H(5) are shifted upfield by the β-CD carvone interaction. However, while the H(5) protons give rise to a relatively broad NMR peak and experience a larger shift, the H(3) signal *gives* a multiplet and its frequency change was difficult to measure due to peak overlapping [4]. Hence, the H(5) NMR signal was used for probing the β-CD carvone interaction. For a D_2O solution of β-CD, i.e., in the absence of guest, the H(5) protons move downfield with increase of temperature (Table I). In addition, for the solutions containing β-CD and each one of the enantiomers, the H(5) chemical shift differences, $\Delta\delta = \delta(\text{free host}) - \delta(\text{host–guest})$, decrease on increasing the host/guest ratio and on raising the temperature (Table II). In fact, these variations reduce the amount of the host–guest complex, thus diminishing the NMR intensity at the host–guest resonance.

No distinct signals ascribed to the free host and the host–guest species could be observed, thus indicating that the fast exchange condition was applicable. For a 300 MHz spectrometer, and a typical value of the largest observed chemical shift difference ($\Delta\delta_{max} \approx 0.3$), the fast exchange condition (i.e., the exchange rate larger than the reciprocal of the largest observed frequency shift in Hz) implies that inclusion and release of the guest should occur at least 90 times/s. Under these conditions, the frequency of a proton signal is obtained by averaging the frequencies of the free host and host–guest species, weighted by their mole fractions [9]. From this relationship, one can easily arrive at $[C]/[\beta\text{-CD}]_0 = \Delta\delta/\Delta\delta_{max}$, showing that $\Delta\delta$ provides a means for measuring the concentration of the host–guest species, [C] [5, 10–12].

Table II. $\Delta\delta$ (ppm) values for H(5) of β-CD, in mixtures of a D_2O solution of β-CD[a] with D_2O solutions of the carvone enantiomers[b], at two different temperatures

$[G]_0$/mM	β-CD.R-Crv		β-CD.S-Crv	
	286 K	318 K	286 K	318 K
5.0	0.147	0.116	0.220	0.037
6.0	0.151	0.130	–	0.054
7.0	0.154	0.141	0.229	0.077
8.0	0.159	0.155	0.231	0.083
9.0	0.165	0.160	0.236	0.111
9.5	0.167	0.171	0.237	0.118

[a] $[\beta\text{-CD}]_0$ = 0.5 mM.
[b] ($[G]_0$ = 5.0, 6.0, 7.0, 8.0, 9.0, 9.5 mM.

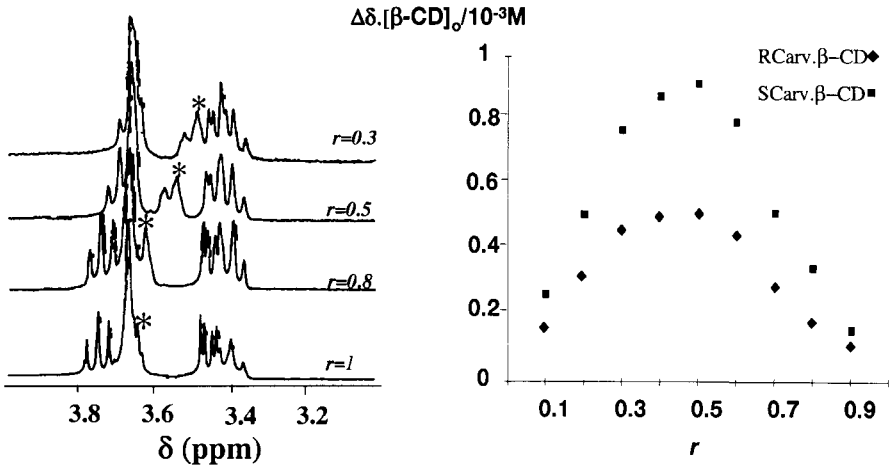

Figure 1. Typical 300 MHz ^{1}H NMR spectra for mixtures of β-CD and R-Crv D_2O solutions with different values of r, in the region of the H(5) signal, and continuous variation plots.

STOICHIOMETRY OF THE HOST–GUEST SYSTEMS

Plotting $\Delta\delta.[\beta\text{-CD}]_0$ for both carvone enantiomers against r leads to maxima at $r \approx 0.5$ (Figure 1), pointing to 1 : 1 stoichiometries [8]. These distributions are roughly symmetrical, suggesting the presence of associations with a single stoichiometry, in this case, of the 1 : 1 type. In fact, competitive formation of associations with distinct stoichiometries would give rise to asymmetric 'Job plots' [8]. In addition, since the appreciably shifted protons in β-CD (H(3) and H(5)) point to the cavity interior, it can be concluded that the host–guest associations are of the inclusion type.

4. Apparent Inclusion Constants at Different Temperatures

The equilibrium for the inclusion process in aqueous solution involves hydrated forms of β-CD and G, and represents a substitution of water molecules in the β-CD cavity by the incoming guest molecule. Hence, the corresponding equilibrium constant is given by $K = K_{app}.a_{H_2O}^{w}$, where a_{H_2O} represents the water activity, the exponent w is the amount of displaced water, and K_{app} is the apparent equilibrium constant which, in this case, measures the extent of inclusion. Introducing the initial concentration conditions (i.e., $[\beta\text{-CD}]_0 = [\beta\text{-CD}] + [C]$, $[G]_0 = [G] + [C]$) in the expression for K_{app}, and making use of $[C]/[\beta\text{-CD}]_0 = \Delta\delta/\Delta\delta_{max}$, one obtains

$$1/\Delta\delta = 1/\Delta\delta_{max} + ([\beta\text{-CD}]_0 K_{app} \Delta\delta_{max})^{-1}([G]_0/[\beta\text{-CD}]_0 - \Delta\delta/\Delta\delta_{max})^{-1}.$$

This equation, exact under the assumption of a single 1 : 1 association equilibrium, represents a linear dependence of $1/\Delta\delta$ vs. $([G]_0/[\beta\text{-CD}]_0 - \Delta\delta/\Delta\delta_{max})^{-1}$, with ordinate intercept given by $1/\Delta\delta_{max}$ and slope by $([\beta\text{-CD}]_0\ K_{app}\ \Delta\delta_{max})^{-1}$. The mathematical solution of this equation, whose unknowns are $\Delta\delta_{max}$ and K_{app}, calls for an iterative recurrence procedure, since one of the unknowns ($\Delta\delta_{max}$) is included in the expression for the independent variable. For the initial concentrations used in this work ($[\beta\text{-CD}]_0$ = 0.5 mM, $[G]_0$ = 5.0, 6.0, 7.0, 8.0, 9.0, 9.5 mM; Table III), $\Delta\delta/\Delta\delta_{max}$ is much smaller than $[G]_0/[\beta\text{-CD}]_0$. In fact, $[G]_0/[\beta\text{-CD}]_0$ takes defined values in the range 10–19, whereas $\Delta\delta/\Delta\delta_{max} < 1$. Hence, the iterative method as applied to the above equation was carried out by successive linear regressions of $1/\Delta\delta$ vs. $([G]_0/[\beta\text{-CD}]_0 - \Delta\delta/\Delta\delta_{max})^{-1}$, with the initial estimate for $\Delta\delta_{max}$ being obtained by neglecting $\Delta\delta/\Delta\delta_{max}$ near $[G]_0/[\beta\text{-CD}]_0$. The iterative convergence of $\Delta\delta_{max}$ to the 3rd decimal place was reached within 2–3 cycles. However, at 301 K and 318 K, appreciable dissociation of β-CD.S-Crv took place (see Table II, for T = 318 K), leading to small $\Delta\delta$ values and to meaningless results when the above equation was used. For instance, for $\Delta\delta$ = 0.054 ppm (value taken from Table II, for β-CD.S-Crv at 318 K, when [S-Crv] = 6.0 mM) with an estimated uncertainty $\pm$10%, and $\Delta\delta_{max}$ = 0.350 ppm, the error amplitude in $1/\Delta\delta$ exceeds $1/\Delta\delta_{max}$. In addition, at these temperatures (301 K and 318 K), the $\Delta\delta$ values for β-CD.S-Crv become roughly proportional to $[G]_0$. This functional dependence between $\Delta\delta$ and $[G]_0$ can be easily derived from the previous general equation by neglecting the terms in $1/\Delta\delta_{max}$, thus yielding $\Delta\delta \approx K_{app}\ \Delta\delta_{max}\ [G]_0$. This equation does not allow separate determination of $\Delta\delta_{max}$ and K_{app}, but only of the product of these quantities.

The results of the above analysis are summarized in Table III. At the two lower temperatures, S-Crv leads to a more stable inclusion compound than its enantiomer (the K_{app} values for the S-Crv inclusion are approximately double of those for β-CD.R-Crv). Being enantiomers, both guest molecules undergo the same solvation processes in aqueous media. Hence, different K_{app} values point to distinct host-guest interactions which, in turn, may lead to enantiomeric discrimination. As the temperature increases, both inclusion systems tend to dissociate, and at 318 K they become appreciably weaker than at room temperature.

Table III. Maximal chemical shift differences for the H(5) protons of β-CD, in mixtures of a D_2O solution of β-CD[a] with D_2O solutions of the carvone enantiomers[b], and apparent association constants for the carvone enantiomers' inclusion in β-CD, at different temperatures. Also given are the number of points (n) and the correlation coefficient (R^2)

T/K	n	R^2	$\Delta\delta_{max}$ (ppm)	$K_{app}/10^2$ M^{-1}
β-CD.R-Crv				
286	6	0.94	0.192	6.8
295	6	0.86	0.208	5.2
301	5	0.90	0.220	3.3
318	6	0.99	0.327	1.1
β-CD.S-Crv				
286	5	0.97	0.256	13.3
293	5	0.91	0.284	10.4
318	6	0.98	0.350[c]	0.5[c]

[a] $[\beta\text{-CD}]_0$ = 0.5 mM.
[b] ($[G]_0$ = 5.0, 6.0, 7.0, 8.0, 9.0, 9.5 mM.
[c] Linear regression with a defined $\Delta\delta$ (see text).

Since the range of temperature values is too short (see "Materials and Experimental Methods") and the number of points scarce, only crude estimates of ΔH^0 and ΔS^0 based on the linear regression of ln K_{app} vs. 1/T could be determined, yielding

β-CD.R-Crv: $\Delta H^0 \approx -43$ kJ mol^{-1}, $\Delta S^0 \approx -90$ J K^{-1} mol^{-1};

β-CD.S-Crv: $\Delta H^0 \approx -81$ kJ mol^{-1}, $\Delta S^0 \approx -220$ J K^{-1} mol^{-1}.

For an appreciable number of β-CD inclusion compounds, it has been previously shown that the corresponding $\Delta H°$ and $\Delta S°$ values fall in one $\Delta H°$-vs.-$\Delta S°$ straight line whose slope, the "compensation" or isoequilibrium temperature, $T_{isoeq} = \Delta(\Delta H°)/\Delta(\Delta S°)$, takes the value 320 ± 30 K [13, 14]. This important general result has been taken as indicating that the inclusion formation is largely independent of the chemical properties of the guest molecule, thus suggesting that one of the driving forces for inclusion is the removal of high-enthalpy water molecules from the cyclodextrin cavity, where these reside in an unfavourable, predominantly hydrophobic environment [15].

Since the $\Delta H°$ and $\Delta S°$ values for the β-CD carvone species are both negative, the inclusion processes become spontaneous for temperatures below T_{isoeq}, assuming that $\Delta H°$ and $\Delta S°$ are constant in the considered temperature range. In addition, these ($\Delta S°$, $\Delta H°$) points fall within the uncertainty range in the general straight line for β-CD inclusion compounds, though the fit is closer for β-CD.R-Crv (Figure 2).

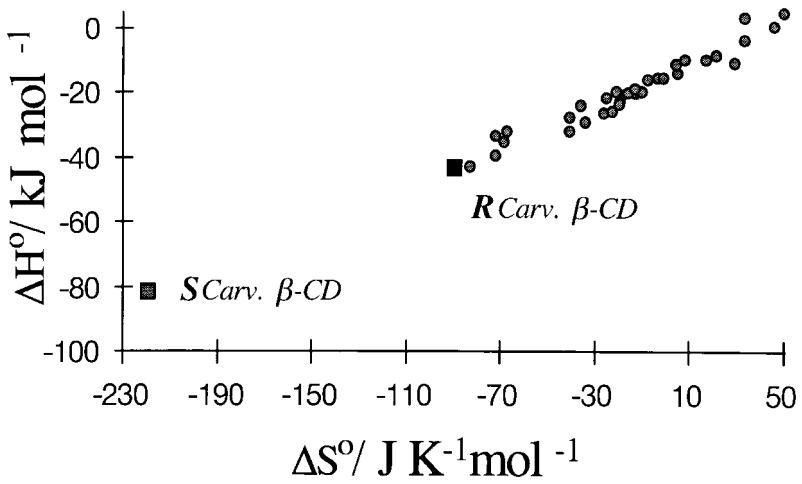

Figure 2. ΔH° vs. ΔS° for β-CD inclusions. The values corresponding to circles were taken from Ref. 14.

The isoenantioselective temperature, $T_{isoen} = \Delta_{R,S}(\Delta H^\circ)/\Delta_{R,S}(\Delta S^\circ)$, is a useful concept for assessing the spontaneity of the *host–(S-guest)* → *host–(R-guest)* process, in particular, when direct competition for inclusion between enantiomers occurs, i.e., when starting with a 50% racemic mixture [16, 17]. For temperatures below T_{isoen} (in the present work, $T_{isoen} \approx 302$ K), the inclusion of the S-Crv form is more stable than β-CD.R-Crv (both $\Delta_{R,S}(\Delta H^\circ)$ and $\Delta_{R,S}(\Delta S^\circ)$ are positive) whereas, at 318 K, β-CD.R-Crv becomes slightly stronger as a result of a larger contribution of the entropic term.

5. Molecular Modelling

Molecular modelling was carried out both at the molecular mechanics and quantum mechanical (semi-empirical and *ab initio*) levels on four model systems: in two of the models (*S-up*, *R-up*), the C=O bonds of the carvone enantiomers were closer to the wider β-CD rim (*up*-orientation), whereas, in the other two (*S-dn*, *R-dn*), the C=O bonds of the carvone enantiomers were closer to the narrower β-CD rim (*down*-orientation).

5.1. MOLECULAR MECHANICS MODELLING

Molecular mechanics results were generated using the program Cerius^{2TM} with the Dreiding force field [18]. The program was developed by BIOSYM/Molecular Simulations. Geometry optimizations were carried out on the above mentioned four model systems in vacuum. Docking of a particular carvone enantiomer inside the β-CD cavity was performed using a Silicon Graphics workstation, by introducing the guest molecule in the β-CD cavity along the vertical axis of the β-CD molecule.

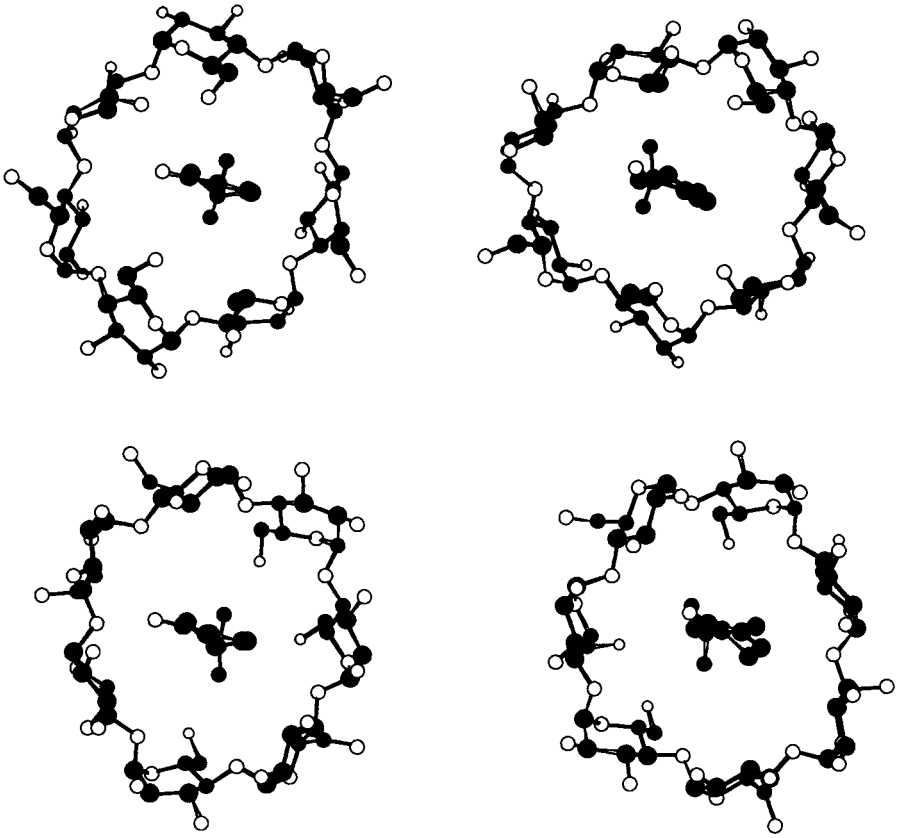

Figure 3. Chem3D views of molecular mechanics structures *S-dn* and *R-dn* (first row), and *S-up* and *R-up* (second row). All the structures present the carbonyl group of carvone closer to the viewer. Hence, in *S-dn* and *R-dn* (first row), the cyclodextrin narrower rim (rim of primary OH groups) is closer to the viewer, whereas in *S-up* and *R-up* (second row), the wider rim of cyclodextrin (rim of secondary OH groups) is the one which is closer to the viewer. H atoms are not shown; C atoms are in black; O atoms are in white.

Figure 3 presents the optimized molecular mechanics structures *S-dn*, *R-dn*, *S-up* and *R-up*. As seen from Table IV, *S*-inclusions are more stable than *R*-inclusions, and *down*-orientations are preferred to *up*-orientations. In addition, the energy partition reveals that the relative stabilization of the *S*-inclusions is mainly due to a lowering of the van der Waals energy (ΔE(vdW)/kJ mol^{-1} (see Table IV): (*R-up*)-(*S-dn*) = 19, (*R-dn*)-(*S-dn*) = 24, (*S-up*)-(*S-dn*) = 11). Also, the R enantiomer does not give any host-guest hydrogen bonding interaction, whereas both orientations of S-Crv inside β-CD have the C=O group of carvone closely interacting with one hydroxyl group of β-CD. In the most stable model compound (S-*dn*), the C=O$\cdots$HO interaction is directed to one primary hydroxyl group of β-CD, C=O$\cdots$HOC(6), with a contact distance of 1.897 Å, the resulting host-guest interaction being stronger than for the S-*up* model compound whose C=O group is

hydrogen bonded to a secondary hydroxyl group HO—C(2) (contact distance of 1.917 Å).

The reduction of the relative stability of β-CD.S-Crv with increase of temperature is consistent with the importance of these hydrogen bonding interactions in explaining the stability of β-CD.S-Crv. In fact, as the temperature increases, these interactions should break, leading to dissociation of the host-guest species.

Another important conclusion emerging from the molecular mechanics results refers to the reorientation of the isopropenyl group inside the β-CD cavity, about the C—C bond linking the ethenyl and asymmetric C atoms. In fact, the optimized structures of the four model compounds have different values for the C=C—C_{as}H dihedral angle (*R-up* = 35°, *R-dn*=7°, *S-up* = 13°, *S-dn* = 1°). This result means that there is enough space within the β-CD cavity for the isopropenyl group to reorient, adopting the more stable orientation in each inclusion compound. Thus, the C=C—C_{as}H dihedral angle acts as a conformational degree of freedom for carvone in the β-CD cavity. Hence, the resulting structures for the guest molecules in the inclusion compounds are no longer exact mirror images of one another, according to the molecular mechanics results.

5.2. QUANTUM MECHANICAL MODELLING

Quantum mechanics calculations were carried out for β-CD and carvone molecules, as well as for model systems of the inclusion compounds, using the Gaussian Program for Windows, G94W [19].

The initial β-CD structure, later partially optimized at the AM1 semi-empirical level, had previously been optimized with a MM+ force field for the inclusion with *p*-dioxan, yielding a rather symmetrical β-CD structure. The AM1 optimization used the following variables: (i) the dihedral angles which define the relative orientations of the individual gluco-pyranose units, (ii) the H—O, O—C bond lengths and the H—O—C bond angles of the secondary hydroxyl groups, and (iii) the HO—CC and OC—CC dihedral angles which define the orientation of the primary hydroxyl groups.

Docking of one carvone enantiomer inside the β-CD cavity was performed using the graphical interface Chem3D program [20], by introducing the guest molecule in the β-CD cavity roughly along the vertical axis of the β-CD molecule. Reversing the sign of one cartesian coordinate of the carvone molecule (x, y or z) produced the corresponding enantiomer. When this transformation was along the molecule's vertical axis (major axis), then the *up* form was additionally reversed to *down*, and vice-versa.

Since computer memory requirements introduced limitations in the use of redundant coordinates in the geometry optimization of the inclusion compounds, multiple scans were performed instead. The following degrees of freedom were considered: (i) rotation about the C2-C5 major axis of the guest, where C5 is the asymmetric carbon atom; (ii) rotation about the C1-C3 axis, where C1 stands for

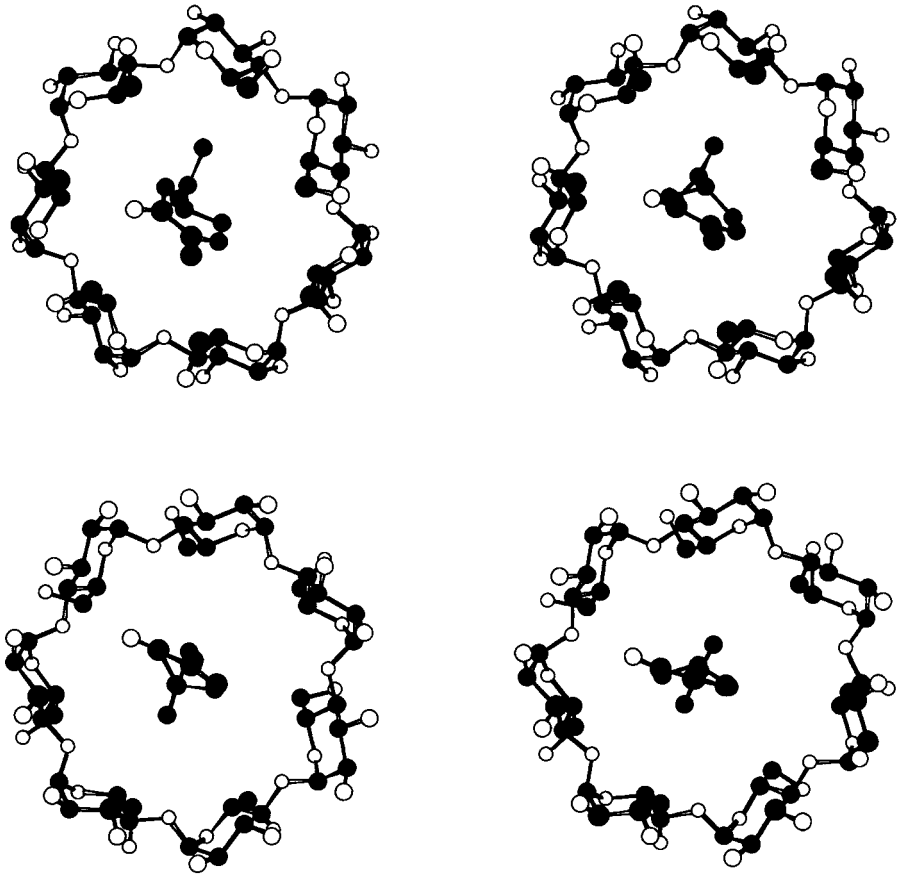

Figure 4. Chem3D views of AM1 model structures *S-dn* and *R-dn* (first row), and *S-up* and *R-up* (second row). All the structures present the carbonyl group of carvone closer to viewer. Hence, in *S-dn* and *R-dn* (first row), the cyclodextrin narrower rim (rim of primary OH groups) is closer to the viewer, whereas in *S-up* and *R-up* (second row), the wider rim of cyclodextrin (rim of secondary OH groups) is the one which is closer to the viewer. H atoms are not shown; C atoms are in black; O atoms are in white.

the carbonyl carbon atom; (iii) horizontal translation of the guest in the β-CD cavity. Different values of these variables were generated using the Chem3D graphical interface [20]. After some preliminary coarse scans of the considered variables, it was found that the scan of variable (i) was decisive in finding the lowest energy configurations corresponding to local minima. The finest variations achieved both in (i) and (ii) were 1°.

After obtaining, in the above mentioned way, the lowest energy configurations for the four model systems considered, single point energy *ab initio* calculations were performed for these configurations, at the STO-3G level, using the Onsager self-consistent reaction field (SCRF) method, with the dielectric constant for water.

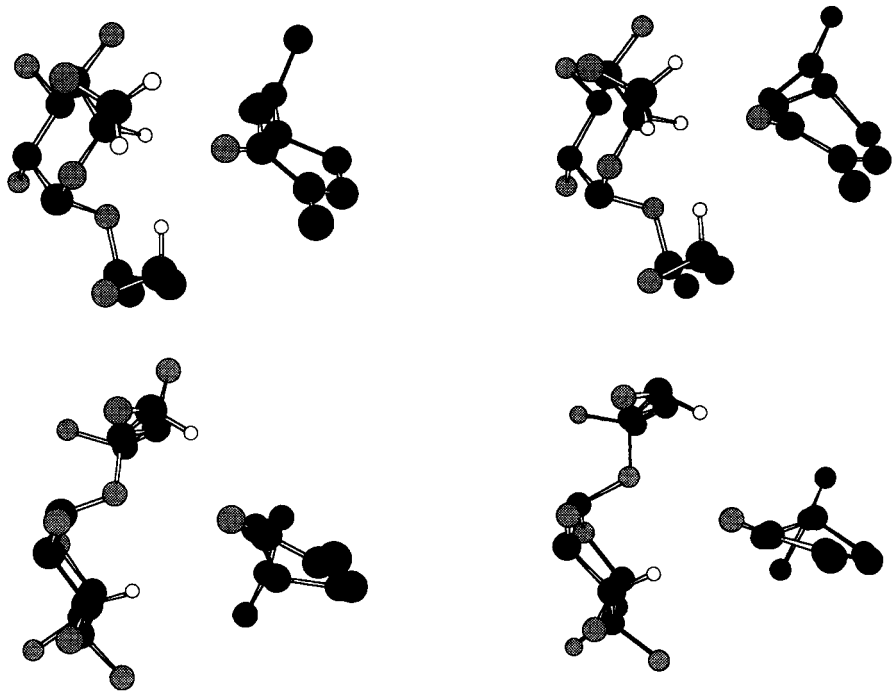

Figure 5. Close-up Chem3D views of the carvone molecule and of the β-CD molecular fragment which is closer to the carbonyl O atom of carvone, for the *S-dn* and *R-dn* (first row), and *S-up* and *R-up* (second row) AM1 inclusion model structures. The H atoms shown (in white) are only those β-CD H atoms which are involved in close attractive contacts ($<$3.0 Å) with the carbonyl O atom of carvone (see Table V). C atoms are shown in black and O atoms in grey. Both *S-dn* and *R-dn* display 4 of these attractive close contacts each, between the carbonyl O atom of carvone and H5, both H6 atoms, and one H6′ atom. In turn, *S-up* and *R-up* exhibit 2 attractive close contacts with H3 and H3' atoms. *R-up* has additionally one repulsive contact with the O(1–4′) atom of β-CD.

Figure 4 shows the location of the carvone enantiomers in the model systems whose structures were determined at the AM1 semi-empirical level. In turn, Figure 5 presents close-up pictures showing the carvone molecules and the cyclodextrin fragments with atoms at distances less than 3.0 Å from the carbonyl oxygen atom of carvone.

As can be seen (Figure 5 and Table IV), both *S-dn* and *R-dn* display four attractive close contacts each, with H5, both H6 atoms, and with the H6′ atom of β-CD. In turn, *S-up* displays two attractive close contacts with the H3 and H3′ atoms of β-CD. On the other hand, *R-up* displays two attractive close contacts with the H3 and H3′ atoms of β-CD, and one repulsive contact with the O(1–4′) atom of β-CD. All of these electrostatic attractions are of the CH$\cdots$O(=) type, involving H atoms which are appreciably positive (Table IV) due to the inductive character of the OH groups linked to the adjacent C atoms. The electrostatic energies associated

Table IV. Value of the C=C—C_{as}H dihedral angle (°), and energies (kJ mol^{-1}) obtained in molecular mechanics calculations for model inclusion systems of the carvone enantiomers in β-CD. Values in parentheses indicate energy differences. C_{as} refers to the asymmetric carbon atom of carvone

C=C—C_{as}H dihedral angle	Bonds	Angles	Torsions	v.d.Waals	Electrostatic	Hydrogen bonds	Total
S-dn							
−1.3	135	284	190	421(0)	87	−87 (−14)	1031 (0)
S-up							
−13.4	117	250	179	432(11)	161	−76 (−3)	1063 (32)
R-dn							
−6.7	118	259	188	445(24)	138	−73 (0)	1077 (46)
R-up							
−35.3	121	266	191	440(19)	140	−76 (−3)	1082 (51)

with these contacts (see Table IV), enable us to understand qualitatively the relative stability of the two more stable model systems, thus pointing out the importance of electrostatic attractive CH$\cdots$O(=) interactions of the hydrogen bonding type in the formation of the inclusion compounds.

Table V summarizes the most relevant *ab initio* STO-3G results. Several conclusions can be extracted from these.

First of all, the relative stability of the model systems as calculated with the STO-3G basis set agrees with the order of stability obtained by the AM1 calculations, though the STO-3G energy separations are much smaller. If the Boltzmann distribution is applied to the energies in solution and the temperature is assumed to be 298 K, then the population of the more stable inclusion model compound (*S-dn*) is 64%, both *R-dn* and *R-up* share 29% of the total population, and the less stable inclusion model system (*S-up*) has the remaining 7%.

Secondly, the differences between the vacuum and the solution energies are small for all the inclusion compounds (<RT at 298 K). The same is true for the inclusion processes in vacuum and in solution. These results seem to suggest that solvation effects due to a solvent represented by a continuum with a particular dielectric constant cannot discriminate among distinct model inclusion systems. However, the relevance of specific solute-solvent interactions, in particular of the hydrogen bonding type, remains open to confirmation and discussion.

The dipole moments for the inclusion model compounds are smaller than the sum of the dipole moments of carvone and β-CD, thus pointing to a partial pairing of dipole moments of carvone and β-CD during inclusion. However, this effect is small and does not seem to correlate clearly with the stability of the inclusion model compounds.

Table V. Atomic charges (atomic units), distances (Å), and electrostatic energies (E_h), obtained at the AM1 level of calculation, for contacts (<3.0 Å) between the carbonyl oxygen atom of carvone and β-CD atoms. Total AM1 energies (E_h) and AM1 energy differences (kJ mol^{-1}) for the model systems in vacuum are also shown for comparison

Model Contacts	q_i	d_{ij}	$\Sigma\, q_i q_j / d_{ij}$	AM1 Energy	Δ(AM1 Energy)
S-dn			−0.0471	−2.64890	0
(C=)O	−0.342				
H5	0.171	2.323			
H6	0.148	2.510			
H6	0.172	2.826			
H6′	0.161	2.407			
R-dn			−0.0441	−2.64718	4.5
(C=)O	−0.339				
H5	0.162	2.549			
H6	0.157	2.403			
H6	0.172	2.822			
H6′	0.149	2.660			
R-up			−0.0083	−2.64353	14
(C=)O	−0.309				
H3	0.188	2.684			
H3′	0.201	2.293			
O(1-4′)	−0.316	2.949			
S-up			−0.0251	−2.64253	17
(C=)O	−0.312				
H3	0.201	2.281			
H3′	0.188	2.953			

Both type of calculations (AM1 semi-empirical and STO-3G *ab initio*) confirm *S-dn* as the more stable model system, in consonance with both the molecular mechanics results and with the experimental results which indicate a preferential inclusion of the S-Crv enantiomer. In addition, the quantum mechanical calculations reveal the importance of multiple CH···O(=) interactions of the hydrogen bonding type for the relative stability of the model systems herein considered. As was previously mentioned, this result is consonant with the reduction of the relative stability of β-CD.S-Crv as the temperature increases.

The molecular mechanics calculations performed allow for full optimization of the model inclusion systems. However, for the calculations carried out at the quantum mechanical level, computer memory requirements drastically restricted

Table VI. Cavity radii (a_0), dipole moments (μ), energies (E), and energy differences (ΔE), for carvone, β-CD and model inclusion systems (see text). Solvation effects are described by the SCRF Onsager method, calculated at the STO-3G *ab initio* level. Solution results (*sol*) were obtained using the dielectric constant for water ($\varepsilon/\varepsilon_0$ = 80.1); *vac* stands for "vacuum" ($\varepsilon/\varepsilon_0$ = 1)

a_0/Å	μ/D		E/E_h		ΔE/kJ mol^{-1}			
	vac	sol	vac	sol	vac	sol	vac–sol	incl.vac–incl.sol
Crv								
4.66	0.9841	1.0953	−455.99012	−455.99090	–	–	2.0	–
β-CD								
7.68	0.8932	0.9774	−4196.42663	−4196.42704	–	–	1.1	–
S-dn								
8.26	1.6643	1.8201	−4652.40234	−4652.40297	0	0	1.7	−1.5
R-dn								
8.06	1.5522	1.7069	−4652.40094	−4652.40156	3.7	3.7	1.6	−1.5
R-up								
7.75	1.2844	1.4346	−4652.40105	−4652.40156	3.4	3.7	1.3	−1.8
S-up								
7.91	1.4289	1.5876	−4652.40038	−4652.40085	5.1	5.6	1.2	−1.9

the number of variables which could be optimized. In particular, only the AM1 semi-empirical calculations allowed a partial optimization of an individual β-CD molecule. For the model inclusion systems, no structural variables of the β-CD or carvone molecule were allowed to vary: only variables concerned with the orientation of the guest molecule in the host cavity were considered in the optimization process of the quantum mechanical calculations. In particular, the orientation of the primary and secondary hydroxyl groups of β-CD were confined to their positions in the individual β-CD molecule. However, it should be mentioned that the full optimization carried out at the molecular mechanics level led to non-symmetrical β-CD structures, thus pointing to the artificial character of the calculation in vacuum.

6. Conclusions

The experimental results herein reported indicate a preferential inclusion of S-Crv in β-CD, both below and at room temperature, a result of theoretical interest for model studies of chiral recognition and of potential pratical application for the food industry. This important result is confirmed by both the molecular mechanics and quantum mechanical calculations herein reported, performed on a set of four model inclusion compounds.

The monocyclic enantiomers considered in this work probably reflect the different stereochemical requirements of the components of a large series of terpenic aromas. The fact that no chiral discrimination is shown by β-CD for these two enantiomers at body temperature and high water activity, which are the normal conditions of use for these monocyclic enantiomers, constitutes additional evidence that β-CD is adequate as a flavour encapsulant for food flavours. As the host-guest interactions which give rise to chiral discrimination are not yet fully understood, this circumstance deserves further investigation.

Acknowledgements

The authors acknowledge support from Junta de Investigação Científica e Tecnológica (J.N.I.C.T.; Project PRAXIS XXI 2/2·1/QUI/17/94) Lisboa. A.M.S. thanks Dr.Teresa Nunes (ICTPOL, Lisboa) and MSc.Ana Isabel Rodrigues (INETI, Lisboa) for help provided during acquisition of NMR spectra.

References

1. J. Szejtli: *Cyclodextrins and their Inclusion Compounds*; Akadémiai Kiadó: Budapest, 1982; D. Duchene: *New Trends in Cyclodextrins and Derivatives*; Editions de Santé: Paris, 1991.
2. G. Jeffrey and W.Saenger: *Hydrogen Bonding in Biological Structures*, Springer Verlag, Berlin, 1991, Chapter 18.
3. V. Schurig and H. Nowotny: *Angew. Chem. Intl. Ed. Engl.* **29**, 939 (1990).
4. J. Redondo, J. Frigola, A. Torrens and P. Lupón: *Mag. Reson. Chem.* **33**, 104 (1995).
5. Y. Bahaddi, H. Galons and N. Rysanek: *Bull. Soc. Chim. Fr.* **32**, 330 (1995).

6. J.E.H. Köhler, M. Hohla, M. Richters and W.A. König: *Angew. Chem. Intl. Ed. Engl*. **31**, 319 (1992).
7. S.M. Han and D.W. Armstrong: In A.M. Krstulovic (ed.), *Chiral Separations by HPLC*, E. Horwood Ltd., Wiley: Chichester, U.K., pp 208–284 (1989).
8. P. Job: *Ann. Chim.* **9**, 113 (1928).
9. H. Günther: *NMR spectroscopy*, 2nd Ed., John Wiley & Sons, Chichester, (1995).
10. P.V. Demarco and A.L. Thakkar: *J. Chem. Soc. Chem. Commun.* **2**, (1970).
11. F. Djedaini, S.Z. Lin, B. Perly and D. Wouessidjeswe: *J. Pharm. Sci*. **79**, 643 (1987).
12. A. Ganza-Gonzalez, J.L. Vila-Jato, S. Anguiano-Igea, F.J. Otero-Espinar, and J. Blanco-Méndez: *Int. J. Pharm.* **106**, 179 (1994).
13. R.J. Clarke, J.H. Coates and S.F. Lincoln: *Adv. Carbohydr. Chem. Biochem.* **46**, 205 (1988).
14. W. Linert, L. Han and I. Lukovits: *Chem.Phys.* **139**, 441 (1989).
15. W. Saenger: *Angew. Chem. Intl. Ed. Engl.* **19**, 344 (1980).
16. K. Watabe, R. Charles and E. Gil-Av: *Angew. Chem. Intl. Ed. Engl*. **28**, 192 (1989).
17. V. Schurig, J. Ossig and R. Link: *Angew. Chem. Intl. Ed. Engl*. **28**, 194 (1989).
18. S.L. Mayo, B.D. Olafson and W.A. Goddard: *J. Phys. Chem.* **94**, 8897 (1990).
19. Gaussian 94, Revision B.2, M.J. Frisch, G.W. Trucks, H.B. Schlegel, P.M.W. Gill, B.G. Johnson, M.A. Robb, J.R. Cheeseman, T. Keith, G.A. Petersson, J.A. Montgomery, K. Raghavachari, M.A. Al-Laham, V.G. Zakrzewski, J.V. Ortiz, J.B. Foresman, C.Y. Peng, P.Y. Ayala, W. Chen, M.W. Wong, J.L. Andres, E.S. Replogle, R. Gomperts, R.L. Martin, D.J. Fox, J.S. Binkley, D.J. Defrees, J. Baker, J.P. Stewart, M. Head-Gordon, C. Gonzalez and J.A. Pople: Gaussian, Inc., Pittsburgh PA, 1995.
20. CS Chem3D Pro(tm), Version 3.5, for Windows 3.1, Windows 95 and Windows NT© 1996, CambridgeSoft Corporation.